ASCA Observations of M82 and NGC 253

ASCA Observations of the Starburst Galaxies M82 and NGC 253

A. Ptak, P. Serlemitsos, & T. Yaqoob
NASA/GSFC LHEA, Code 662

Abstract

We present the results of ASCA observations of M82 and NGC 253. The ASCA spectra of NGC 253 are fit well with a power-law ($\Gamma \sim 2.0$) + thermal Raymond-Smith plasma (kT ~ 0.8 keV) model. While this model also gives an acceptable fit to the M82 spectra (with kT ~ 0.65 and $\Gamma \sim 1.8$), the best-fitting model for M82 is a combination of three thermal Raymond-Smith components (with kT ~ 0.4, 1.1 and 12.4 keV, as reported by Tsuru et al. 1995), although substituting a power-law for the hard component ($\Gamma \sim 1.7$) results in only a slightly higher value of χ^2. In both M82 and NGC 253 all components are absorbed in excess of the galactic values, with soft (and medium) component absorption on the order of 10^{21} cm^{-2} and hard component absorption on the order of 10^{22} cm^{-2}. The thermal components in both galaxies require abundances that are significantly subsolar. The ratio of Fe to O, Mg, Si and S abundance in the soft component of NGC 253 and the soft and medium components of M82 is ~ 0.1-0.2, implying a contribution from massive stars (i.e., a top-heavy IMF) if the emission is due to disk and/or halo gas. An upper limit on Fe-K emission in NGC 253 can be set at an equivalent width (EW) of ~ 180 eV at 6.7 keV and 220 eV at 6.4 keV. Fe-K emission at 6.63 (6.41-6.75) keV with an EW of 94 (37-155) eV is marginally significant in M82. The compactness, low level of Fe-K emission, and possible variability above 2 keV suggests the hard component may have a significant non-thermal contribution, probably from several blackhole candidates with M > 10 solar masses. M82 and NGC 253 are (spectrally) very similar to other starbursts, LINERs and low-luminosity AGN observed by ASCA.

Spectral Fitting

Table 1 shows the results of fitting the SIS spectra within 3’ and 6’ regions (using PI values from S0 chips 1 & 2 and S1 chips 0 & 3) and GIS spectra within 4’ and 6’ regions (for both SIS and GIS spectra, the background was subtracted using counts in an annulus around the sources with an inner radius of 6.5’) with simple power-law and Raymond-Smith models. While the SIS spectra clear reject a single-component model, both a power-law and a Raymond-Smith are acceptable to the GIS spectra. Figure 1 shows the residuals from the simple power-law fit to the SIS spectra, with strong line emission clearly present. Adding an addition component gives acceptable fits (shown in figure 2). Adding a third component further improves the M82 fits (primarily due to fitting the Si Ly_α line at 2.00 keV and excesses around 6-7 keV), while a third component does not contribute significantly to the NGC 253 fits (shown in figure 3). The results of the two-component NGC 253 fits and two and three-component M82 fits are shown in tables 2 and 3 , respectively, where it can be seen that all abundances are significantly subsolar. A narrow Gaussian at 6.63 (6.41-6.75) keV with an EW of 94 (37-155) eV reduces χ^2 by 12.8 in the power-law + Raymond-Smith M82 fit, significant at only the 3σ level. An upper limit on Fe-K emission in NGC 253 can be set at an EW of ~ 180 eV at 6.7 keV and 220 eV at 6.4 keV. The weak Fe-K emission in both M82 and NGC 253 constrains the hard component abundance to be significantly sub-solar.

Table 1: Single-component fits to ASCA Spectra

Galaxy	Det.	Model[a]	N_H[b]	Γ/kT (keV)	A[†]	χ^2/dof
NGC 253	S0-1[c]	PL	1.2	1.93		415.6/257 = 1.62
NGC 253	S0-1[c]	R-S	0.4	4.9	0.0	426.3/257 = 1.65
NGC 253	S2-3[d]	PL	0.4 (<1.5)	1.87 (1.77-2.00)		397.2/420 = 0.95
NGC 253	S2-3[d]	R-S	0.0 (<0.3)	5.4 (4.8-6.3)	0.12 (<0.4)	403.7/419 = 0.96
NGC 253	S2-3[e]	PL	0.9 (0.0-2.0)	1.93 (1.81-2.07)		505.4/508 = 0.99
NGC 253	S2-3[e]	R-S	0.0 (<0.4)	5.2 (4.6-6.0)	0.06 (<0.3)	510.8/507 = 1.01
M82	S0-1[c]	PL	1.5	1.80		1357/411 = 3.30
M82	S0-1[c]	R-S	0.8	7.1	0.2	1465/410 = 3.57
M82	S2-3[d]	PL	0.0 (<0.2)	1.61 (1.58-1.65)		890.9/849 = 1.05
M82	S2-3[d]	R-S	0.0 (<0.1)	9.6 (8.7-10.8)	0.3 (0.1-0.5)	943.9/848 = 1.11
M82	S2-3[e]	PL	0.0 (<0.1)	1.63 (1.59-1.66)		969.8/910 = 1.07
M82	S2-3[e]	R-S	0.0(<0.1)	9.3 (8.5-10.4)	0.3 (0.1-0.4)	1053/909 = 1.16

Parentheses give 90% confidence intervals for two interesting parameters (only computed for fits with $\chi_\nu^2 < 1.5$).

[a] PL = Power-law; R-S = Raymond Smith   [b] x 10^{21} cm^{-2} [†] Relative to solar

[c] 3’ source region using PHA values   [d] 4’ source region   [e] 6’ source region

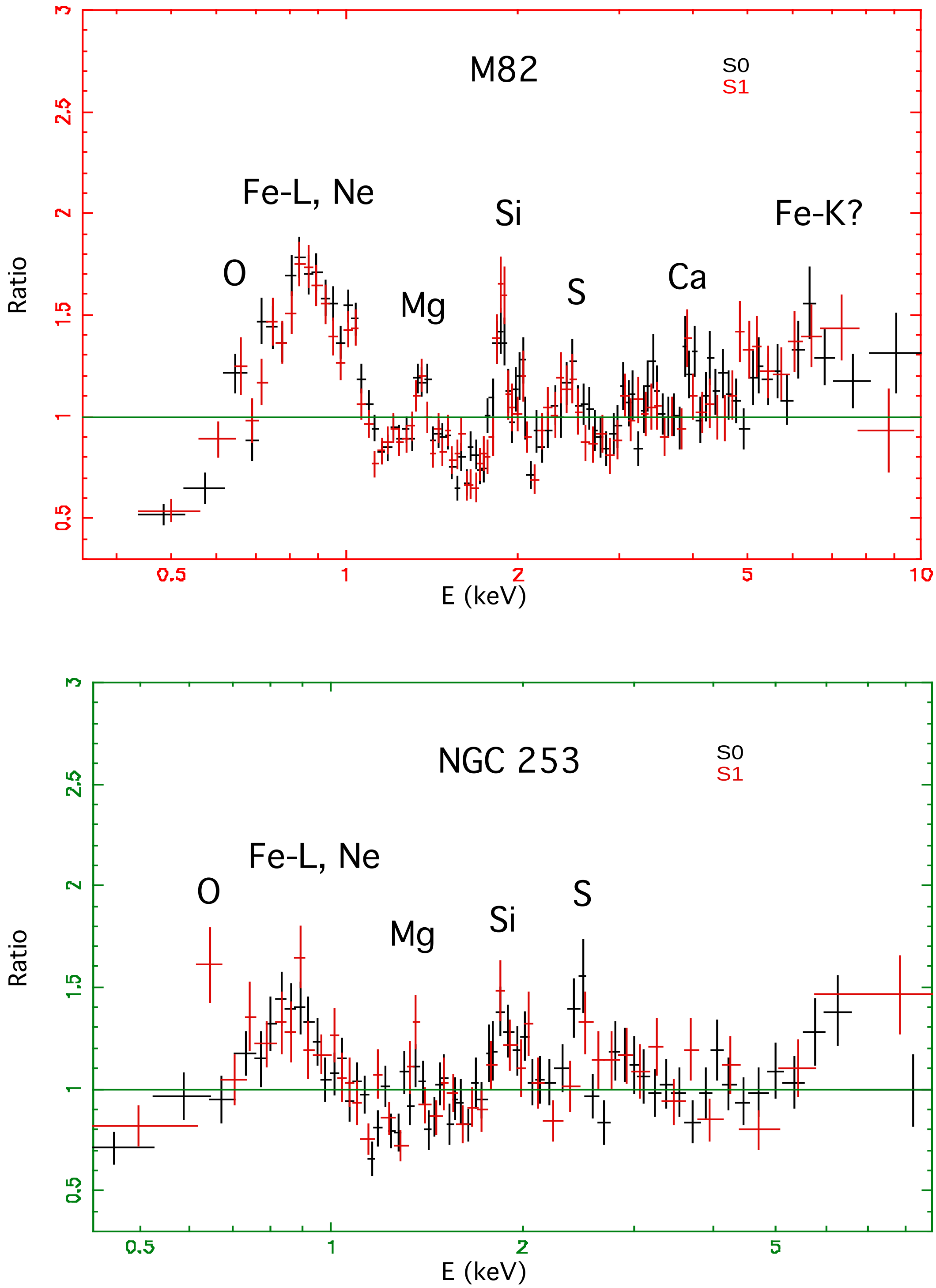

Figure 1: Ratio of data/model for a simple power-law fit (with absorbtion) fit to M82 (top) and NGC 253 (bottom).

Table 2: Two-component Fits to *ASCA* NGC 253 Spectra

Det.	Model (soft/hard)	N_H[a]	kT (keV)	A†			N_H[b]	Γ/kT (keV)	A†	χ^2/dof
				N, Ne, Ar, Ca, Fe, Ni	O, Mg, Si, S					
S0-1 (3')[c]	R-S/PL	1.3 (0.8-2.6)	0.80 (0.74-0.84)	0.06 (0.03-0.19)	0.33 (0.21-0.97)		15 (5-26)	2.01 (1.72-2.36)		326.1/291 = 1.12
S0-1 (3')[c]	R-S/R-S	0.9 (0.0-1.7)	0.80 (0.74-0.84)	0.08 (0.03-0.26)	0.44 (0.23-1.52)		7 (4-12)	7.1 (1.8-16.8)	0.14 (0.00-0.36)	328.6/290 = 1.13
S0-1 (6')[d]	R-S/PL	1.0 (0.1-1.5)	0.80 (0.75-0.84)	0.05 (0.03-0.12)	0.29 (0.19-0.57)		15 (7-23)	2.03 (1.74-2.37)		417.7/361 = 1.16
S0-1 (6')[d]	R-S/R-S	0.8 (1.4-0.0)	0.80 (0.75-0.84)	0.07 (0.03-0.16)	0.36 (0.11-0.84)		8 (3-15)	7.1 (5.0-10.8)	0.03 (0.00-0.19)	424.9/360 = 1.18
S0-3 (6')[e]	R-S/PL	1.0 (0.1-1.5)	0.79 (0.75-0.84)	0.05 (0.03-0.12)	0.28 (0.18-0.55)		14 (7-22)	2.03 (1.84-2.24)		915.4/871 = 1.05
S0-3 (6')[e]	R-S/R-S	0.8 (0.0-1.4)	0.80 (0.75-0.84)	0.06 (0.03-0.15)	0.35 (0.21-0.82)		8 (3-14)	7.1 (5.5-9.5)	0.02 (0.00-0.15)	923.4/870 = 1.06
				N, Ar, Ca, Ni	O, Mg, Si, S	Ne, Fe				
S0-3 (6')[e]	R-S/PL	1.0 (0.5-1.9)	0.80 (0.73-0.84)	<0.25	0.27 (0.18-0.55)	0.05 (0.03-0.12)	14 (7-22)	2.01 (1.83-2.23)		915.0/870 = 1.05
S0-3 (6')[e]	R-S/R-S	0.8 (0.0-1.4)	0.81 (0.75-0.84)	<0.23	0.34 (0.21-0.83)	0.07 (0.03-0.16)	8 (3-14)	7.3 (5.6-9.9)	0.02 (0.00-0.15)	922.3/870 = 1.06

Parentheses gives 90% confidence intervals for two interesting parameters ($\Delta\chi^2 = 4.605$).

† Relative to solar

[a] X 10^{21} cm^{-2}, applied to entire model

[b] X 10^{21} cm^{-2}, applied to hard component only

[c] 3' region using PI values from S0 chips 1 & 2 and S1 chips 0 & 3

[d] 6' region using PI values from S0 chips 1 & 2 and S1 chips 0 & 3

[e] SIS as in [d], 6' GIS region

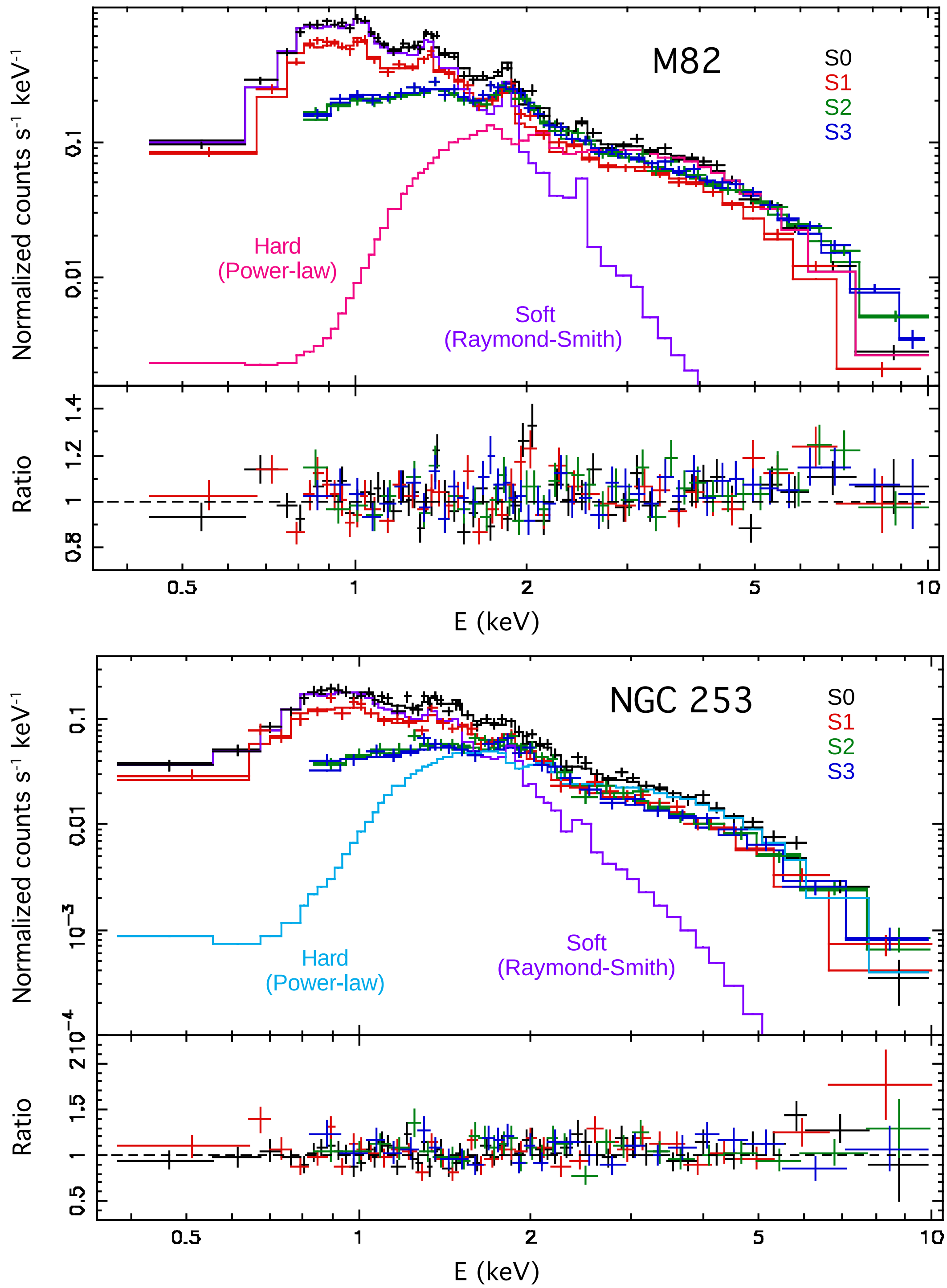

Figure 2: Power-law + Raymond-Smith fits to ASCAM82 (top) and NGC 253 (bottom) spectra. The hard and soft components from the S0 fits are shown.

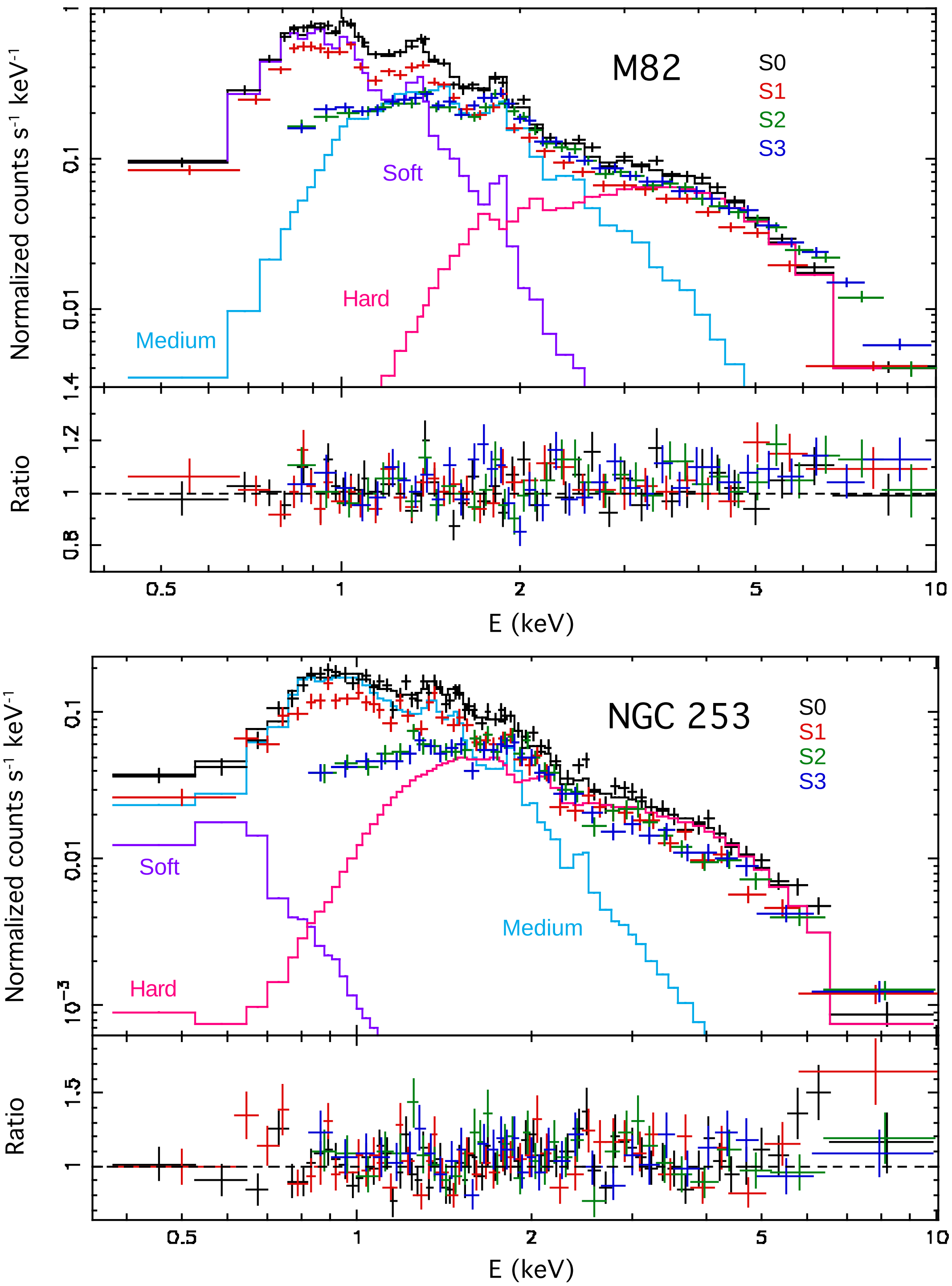

Figure 3: Raymond-Smith + Raymond-Smith + Raymond-Smith fits to *ASCA*M82 (top) and NGC 253 (bottom) spectra. The model (with soft, medium, and hard components shown separately) is shown for S0 only (for clarity).

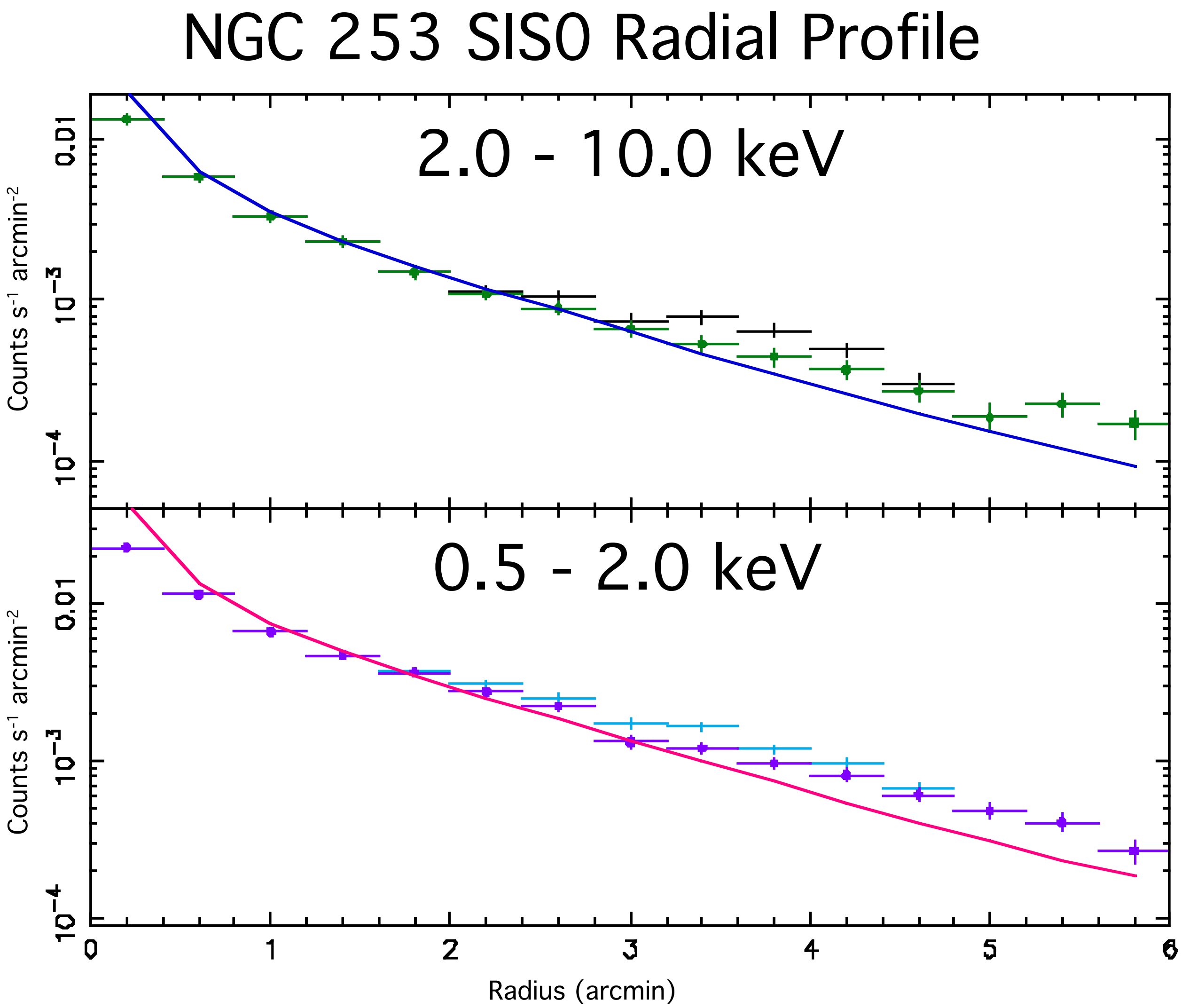

Figure 4: Radial profile of NGC 253 in the 2-10 keV (top) and 0.5-2.0 keV (bottom) bands. The marked points show the result of removing four extranuclear point sources (by excluding all counts within 1' of the PSPC positions of the sources). The solid lines show the XRT PSF normalized to the profiles with point sources excluded. It is evident that the four point sources contribute significantly to the "extended" flux of NGC 253 above 2 keV. The SIS profiles of M82 show that the flux above 2 keV is not extended (Tsuru, *et al.*1995). This suggests that in both M82 and NGC 253 there is a significant point source contribution to the 2-10 keV flux.

Table 4: *ASCA* Fluxes and Luminosities for M82 and NGC 253

Galaxy	Energy Range	Observed Flux (x 10^{-12} ergs s^{-1} cm^{-2})	Absorption-Corrected Luminosities (x 10^{40} ergs s^{-1})				
			Two-component Fit†		Three-component Fit*		
			Soft	Hard	Soft	Medium	Hard
M82	0.5-2.0 keV	9.4	2.7	2.1	3.2	2.5	1.4
M82	2.0-10.0 keV	20	0.20	3.5	0.02	0.61	3.4
NGC 253	0.5-2.0 keV	2.9	0.23	0.33	0.02	0.26	0.19
NGC 253	2.0-10.0 keV	4.6	0.03	0.37	0.00	0.03	0.35

All values are averages from S0-3 fits (fluxes of individual instruments are within 4% of the mean).
Observed fluxes are from three-component fits (two-component fits give similar results).
† Power-law (hard) + Raymond-Smith (soft)
* Raymond-Smith + Raymond-Smith + Raymond-Smith

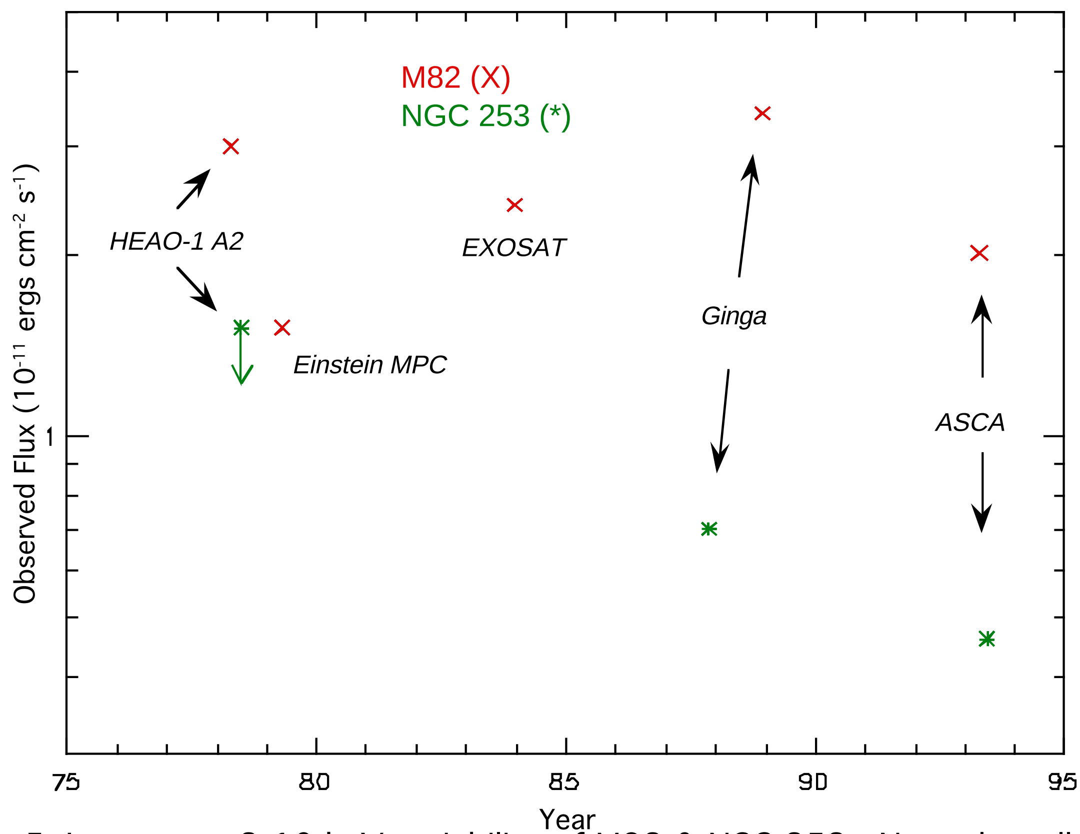

Figure 5: Long-term 2-10 keV variability of M82 & NGC 253. Note that all values prior to *ASCA* are from *non-imaging* detecors.

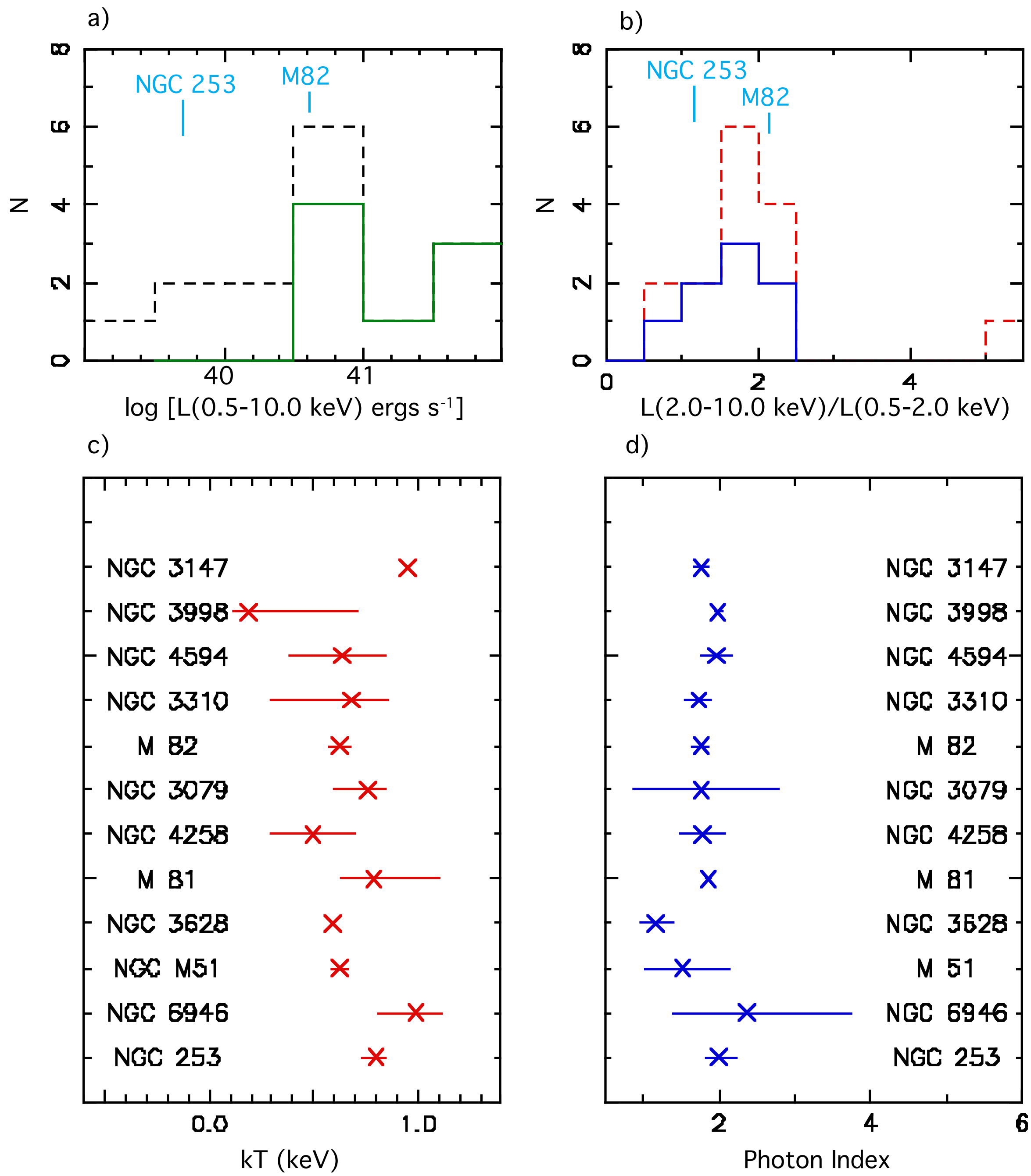

Figure 6: Comparison of M82 and NGC 253 with other low-activity galaxies observed by *ASCA*[shown in c) and d); see Serlemitsos, *et al.*(1995)]. **a)** Observed ASCA luminosty (solid line shows LINERs/LLAGN only), with the M82 and NGC 253 values marked. **b)** As in a) with hardness ratio. **c)** kT measured from power-law + Raymond-Smith model (arranged in order of increasing L_X). **d)** As in c) with photon index.

Discussion

1. *The Nature of the Hard Component*

Recent modeling (Suchkov *et al.* 1994) predicts that if the hard component in starburst galaxies is due to the *direct* emission from "superwinds" then a) the observed abundances should high (i.e., enriched by supernovae) and b) the hard component luminosity should be about an order of magnitude lower than the soft component luminosity. Gas with a temperature of ~ 6 keV and solar Fe abundances should have a strong Fe line at 6.7 keV with an EW of ~ 900 eV (Rothenflug & Arnaud 1985). Our luminosities (*table 4*) and Fe-K EW limits show that a significant superwind contribution to the hard component is unlikely in both M82 and NGC 253. The radial profiles of NGC 253 (*figure 4*) and M82 (Tsuru *et al.* 1995) and possible variability (*figure 5*) suggest a significant point source contribution in both M82 and NGC 253 above 2 keV. It is likely that the hard component in these galaxies is predominately non-thermal, resulting primarily from several X-ray binaries with M > 10 solar masses (i.e., blackhole candidates). A highly-absorbed AGN and (possibly) also from inverse-Compton scattering of IR photons by relativistic electrons (note that a 6 kpc-scale radio synchrotron halo has been observed in NGC 253; Carilli *et al.* 1992) may also be contributing.

2. *The Nature of the Soft and Medium Components*

The soft and medium components in M82 and NGC 253 have temperatures and luminosities consistent with a starburst origin (Suchkov *et al*. 1994; Tomisaka & Bregman 1993). The morphology of the X-ray flux in 1/4, 3/4 and 1 1/4 keV *PSPC* bands suggests that the soft component is due to emission coincident with their halos (along the minor axes) while much of the medium component is coincident with their (galactic) disks (c.f., Dahlem, Weaver, & Heckman 1996). The low abundances suggest that the ambient disk and halo gas had not been enriched prior to any starburst-related shock heating. However, the underabundance of Fe relative to O, Mg, Si, and S may be indicative of an IMF biased towards massive stars (c.f., Mushotzky *et al.* 1996). Some of the medium component may also be due to the direct emission of several Type II supernova remnants.

3. Relation of M82 and NGC 253 to Other Low-Activity Galaxies

Figure 6 shows that M82 and NGC 253 are *not* conspicuous compared to other starburst, LINER and low-luminosity AGN galaxies with respect to their luminosities and spectral shape. This suggests that many galaxies have hot ISM heated via starburst mechanisms similar to those at work in M82 and NGC 253 (note the similarity of the observed temperatures when the galaxies are fit with a two-component spectrum). The rather narrow range of hard component photon indices may be the result of an ubiquitous accretion-driven component (i.e., obscured AGN or luminous X-ray binaries) in these galaxies.

References

Carilli, C., Holdaway, M., Ho, P., & DePree, C. 1992, ApJ, 399, L5
Mushotzky, R. et al., ApJ, submitted
Rothenflug, R., & Arnaud, M. 1985, A & A, 144, 431
Serlemitsos, P., Ptak, A., & Yaqoob, T. 1995, in *The Physics of Liners*, in press
Suchkov, A. Balsara, D., Heckman, T., & Leitherer, C. 1994, ApJ, 430, 511
Tomisaka, K. & Bregman, J. 1993, PASJ, 45, 513
Tsuru, T. et al. 1995, in *Maryland October Conference: Cosmic Abundances*, in press